SIN-CHN SCIENTIFIC PRESS PTE.LTD.

Molecular & Cellular Biomechanics 2025, 22(2), 800.
https://doi.org/10.62617/mcb800

Article

Biomechanical optimization of RGB LED systems: Temperature prediction model and optical compensation algorithm based on built-in constant current source chip

Liangjie Tao, Miao Liu*

Shanghai University of Engineering Science, Shanghai 201620, China
*** Corresponding author:** Miao Liu, liumiao@sues.edu.cn

CITATION

Tao L, Liu M. Biomechanical optimization of RGB LED systems: Temperature prediction model and optical compensation algorithm based on built-in constant current source chip. Molecular & Cellular Biomechanics. 2025; 22(2): 800. https://doi.org/10.62617/mcb800

ARTICLE INFO

Received: 14 November 2024
Accepted: 22 November 2024
Available online: 10 February 2025

Abstract: In the realm of modern applications, especially those related to human - involved scenarios such as vehicles and medical or wearable devices, the performance of RGB LED lights is of great significance. Beyond the traditional concerns of electronic - optical properties, the integration of biomechanics - related factors can bring new perspectives and optimizations. In vehicles, during prolonged illumination, the color shifts of various LED lights not only affect driving comfort but also have potential implications for driving safety from a biomechanical perspective. The human body's visual and psychological responses to these color and luminance changes are complex. For example, sudden or inconsistent color changes can cause visual fatigue and distraction, which may impact a driver's reaction time and decision - making ability, all of which are related to biomechanical aspects of human - machine interaction. Each LED shows deviations in wavelength and luminous intensity, and the light decay of RGB chips is inconsistent. To address these issues and ensure consistent color and luminance of all RGB ambient lights during use, this paper proposes a temperature prediction model (PT - model) based on constant current source output PWM. This model takes into account the impact of temperature changes on the color coordinates and luminous flux of LED lights. Moreover, considering the potential applications in medical and wearable devices, the model's performance becomes even more crucial. In medical light - based treatment devices, the precise control of RGB LED temperature and light output is essential for ensuring the effectiveness of treatment while minimizing potential harm to human tissues. Biomechanics research can provide insights into how different tissues respond to light - induced heat and mechanical stress. Similarly, in wearable devices for health monitoring, the stability of RGB LED performance is related to the comfort and accuracy of the device's operation on the human body. Experimental results show that compared to traditional models, the prediction accuracy of this model is significantly improved, with errors reduced to within 4.3%. The model's effectiveness is verified under different ambient temperatures ranging from −40 ℃ to 120 ℃, which is crucial for ensuring its reliability in various real - world applications, especially those related to human - centered scenarios influenced by biomechanical factors.

Keywords: RGB LED; temperature compensation model; PWM control; optical algorithm; light color consistency

1. Introduction

In modern automotive design, interior ambient lighting is not only a crucial means of enhancing the aesthetics of the cockpit, but also plays a pivotal role in creating a comfortable driving environment and enhancing the visual experience of the driver. However, over prolonged use, the issue of color shift in interior RGB ambient lighting has become increasingly prominent, becoming a significant factor

affecting driving comfort and safety [1–3]. This color shift primarily stems from individual differences in LED wavelength and light intensity, as well as inconsistencies in the light decay rate of the three RGB color chips.

Traditional temperature models exhibit significant limitations in predicting the temperature of LED lights. These models often focus solely on the performance description of a single LED light, neglecting the complex interactions between LED self-heating, electronic component self-heating, and heat transfer on the PCB board. Firstly, traditional models fail to fully consider the impact of LED self-heating on temperature, which directly leads to insufficient prediction accuracy [4–6]. Secondly, these models typically rely solely on the LED heating characteristic curves provided in the specifications, neglecting the dynamic heating characteristics of LEDs during power-on, thus failing to accurately reflect the actual operating temperature of LEDs. Furthermore, traditional models also appear to be inadequate in dealing with temperature prediction issues when multiple LEDs are mixed, especially in high-temperature environments where the proportion of temperature interaction between channels becomes uncertain, further increasing the error in temperature calculation [7].

This article aims to propose a temperature prediction model (PT-model) based on constant current source output PWM, in order to overcome the limitations of traditional models. By deeply analyzing the characteristics of LED lamps changing with temperature and fully considering the self-heating and heat transfer effects of LEDs, for example **Figure 1** this model achieves accurate prediction of the actual temperature of LED lamps [8]. On this basis, by dynamically adjusting the PWM signals of RGB channels in combination with optical algorithms, it effectively compensates for the shifts in color coordinates and luminous flux caused by temperature changes, significantly improving the light color stability and consistency of interior ambient lighting. The research in this article not only fills the gaps in prediction accuracy and application scope of existing temperature models, but also provides strong theoretical support and practical guidance for enhancing the performance of interior lighting systems and improving the driving experience.

2. Construction of a temperature prediction model (PT-model) based on constant current source output PWM

2.1. Overview of traditional temperature models

Traditional LED temperature prediction technology, rooted in the physical characteristics and thermal principles of LEDs, relies on thermal resistance network models and Fourier heat conduction theory to build an accurate temperature prediction framework. However, despite demonstrating certain predictive capabilities in specific scenarios, its inherent limitations cannot be ignored [9].

Specifically, traditional models primarily rely on the LED heating characteristic curves provided in the specifications to predict the temperature of a single LED. Although they may exhibit high accuracy in predicting the temperature of a single LED, these models struggle to directly predict the overall temperature after mixing three LEDs. Especially in high-temperature environments, the proportion of mutual

influence between channels becomes uncertain, leading to increased errors in temperature calculation and subsequently affecting the consistency of light color to some extent. Furthermore, traditional models overlook the dynamic heating characteristics of LEDs during power-on [10]. They only indirectly estimate the LED temperature by reading the MCU temperature, but this approach does not accurately reflect the actual operating temperature of the LED [11]. Therefore, the model may have deficiencies in color coordinate shift and PWM duty cycle adjustment, which ultimately may lead to inconsistent light color.

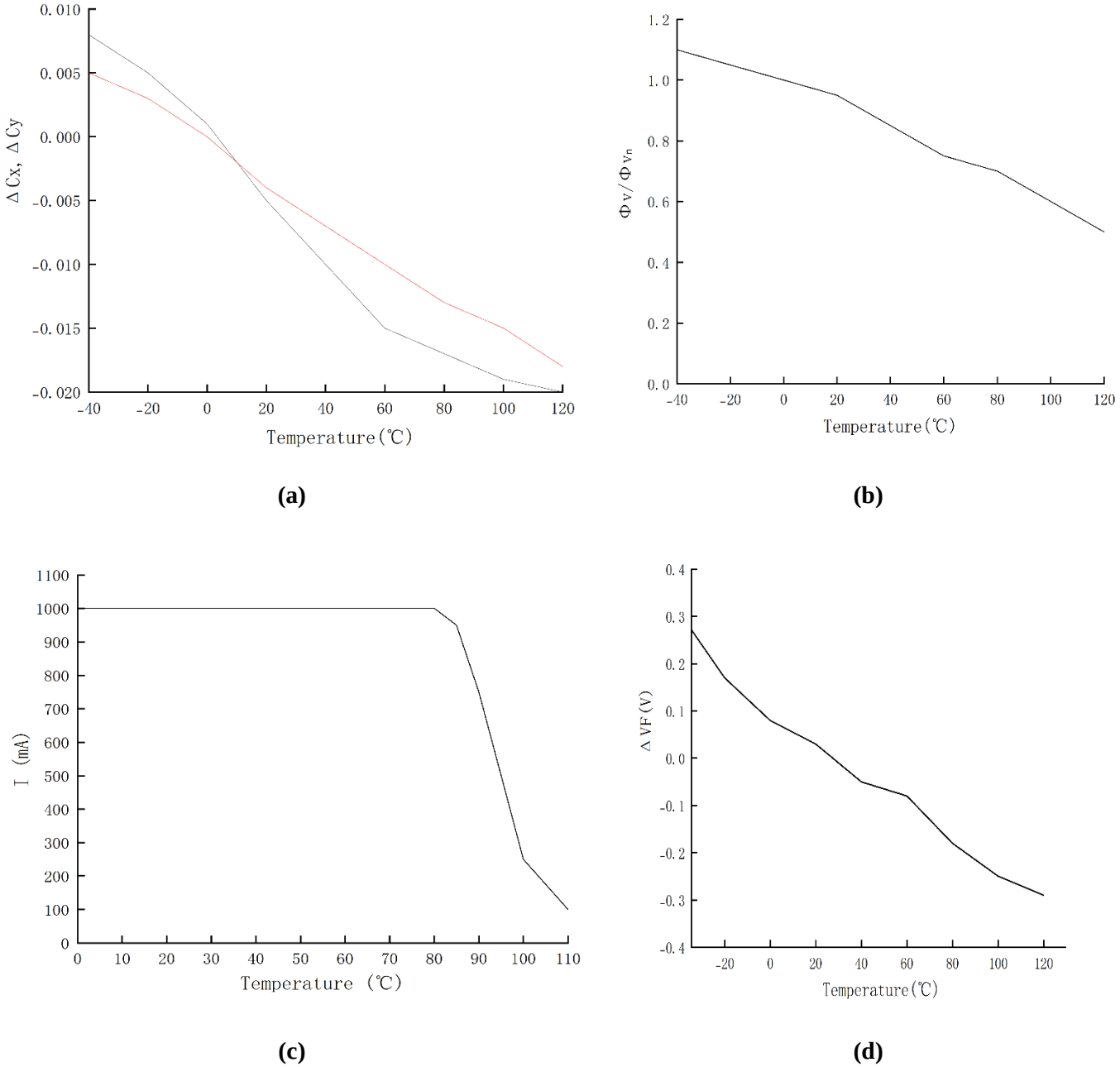

Figure 1. Variation of color coordinates, luminous flux, current, and voltage of a single LED with temperature. **(a)** Variation of color coordinates of a single LED with temperature; **(b)** Variation of luminous flux of a single LED with temperature; **(c)** Current of a single LED varies with temperature; **(d)** Voltage of a single LED varies with temperature.

2.2. Recent advancements and challenges of machine learning in LED temperature prediction

In recent years, with the rapid development of machine learning technology, its application in the field of LED temperature prediction has gradually increased [12,13]. Machine learning-based prediction methods typically involve collecting a large amount of LED working data and training models using algorithms such as neural networks and support vector machines to achieve LED temperature prediction. These methods can handle complex nonlinear relationships and mine potential patterns in data, theoretically achieving higher prediction accuracy. However, machine learning methods still face many challenges in practical applications. Firstly, model training requires a large amount of high-quality data, which incurs high costs for data acquisition and processing. The generalization ability of the model is limited by the coverage range of the training data, and the prediction accuracy may significantly decrease for unseen working conditions or LED models. Machine learning models have high computational complexity and high requirements for hardware resources, making it difficult to deploy them in resource-constrained embedded systems.

2.3. Innovation and advantages of PT-model

In response to the limitations of traditional LED temperature prediction techniques and the challenges posed by machine learning methods, this paper introduces an innovative temperature prediction model (PT-model) for RGB LEDs based on a built-in constant current source chip. This model exhibits significant advantages in the following aspects:

Multi-physical field coupling modeling. The PT-model comprehensively considers various heat transfer modes of LEDs, such as thermal conduction, convection, and radiation, as well as the coupled effects of multiple factors, including LED self-heating, electronic component self-heating, and PCB board thermal conduction. By introducing the modified Fourier's law of heat conduction and thermal resistance equation, a more accurate multi-physical field coupling model is established.

Dynamic thermal effect analysis. In response to the dynamic thermal effect generated by LEDs during operation, the PT-model introduces the concept of time step, conducting a dynamic analysis of the heat accumulation and dissipation processes of LEDs under different duty cycles. Through iterative calculations, real-time and high-precision prediction of LED temperature is achieved.

Adaptability to complex thermal environments. For complex systems with multiple LEDs for mixed lighting, the PT-model accurately describes the thermal coupling effects between LEDs and the thermal conduction paths of the PCB board by constructing a thermal network model. At the same time, the model also considers the impact of factors such as ambient temperature changes and differences in heat dissipation conditions on LED temperature, improving the accuracy and reliability of prediction results.

Computational efficiency and resource optimization. Compared to machine learning methods, PT-model significantly reduces computational complexity and has looser requirements for hardware resources. This makes the model easier to deploy

and apply in practical engineering environments, especially excelling in resource-constrained embedded systems.

2.4. PT-model construction

2.4.1. Overview of PT-model

The PT-model constructed in this article is a temperature prediction model specifically designed to address the issue of inconsistent light color under temperature variations in RGB LED ambient lights. During the temperature prediction process for LED mixed light, significant errors can occur when the temperature change of a single LED leads to a prediction of mixed light temperature. Therefore, in the temperature calculation model, to enhance the accuracy of LED mixed light temperature prediction, the PT-model is constructed based on LED specifications and a wealth of experimental data. The PT-model comprehensively considers multiple factors such as LED self-heating, electronic component self-heating, and heat transfer of the PCB board. Its aim is to provide a reliable basis for subsequent dynamic compensation of color coordinates and luminous flux by accurately predicting the actual operating temperature of LEDs. The innovation of the PT-model lies in its integration of Fourier's law of heat conduction, thermal resistance equation, and the characteristics of constant current source output PWM signal, achieving real-time and dynamic prediction of LED temperature, significantly improving the accuracy and practicality of prediction.

2.4.2. PT-model construction process

In the process of predicting LED mixed light temperature, when a single LED temperature change leads to the prediction of mixed light temperature, a significant error may occur in the mixed light temperature. Therefore, in the temperature calculation model, in order to improve the accuracy of LED mixed light temperature prediction, the construction of the PT-model is based on LED specifications and a large amount of experimental data [14]. Firstly, the mathematical relationship between LED heat generation, power, and ambient temperature was established through Fourier's law of heat conduction and the thermal resistance equation. Secondly, to eliminate the superimposed effects of self-heating of electronic components and heat transfer of the PCB board, this paper innovatively proposes a new measurement method. Specifically, the electronic components are separated from the PCB board and connected using wires to test the temperature of the soldering pad. Based on this method, the expression for the temperature difference in heat conduction is revised, and an equation for calculating the actual temperature of the LED is derived [15]. Finally, leveraging the characteristics of constant current source output PWM, a PT-model was established to achieve precise prediction of LED temperature. The details are as follows:

The expression for the self-heating power of an electronic component in relation to its input and output power is:

$$P_{origin\_t} = P_{origin\_in} - P_{origin\_out} \tag{1}$$

In the equation P_{origin_t} represents self-heating power, P_{origin_in} represents the input power of the heating source, P_{origin_out} represents the output power.

The expression for P_{origin_out} is:

$$P_{origin\_out} = \eta P_{origin\_in} \tag{2}$$

η represents mechanical efficiency. Therefore, the self-heating power P_{origin_t} of electronic components can be replaced by the following equation:

$$P_{origin\_t} = (1 - \eta) P_{origin\_in} \tag{3}$$

According to Fourier's law of heat conduction:

$$Q_{cond} = \frac{kA\Delta T_{cond}}{d} \tag{4}$$

In the equation k represents thermal conductivity, which is related to the material and can be obtained through experiments, In the equation, A represents the cross-sectional area for heat conduction, d represents the length or thickness of the thermal conduction path, ΔT_{cond} the expression for calculating the thermal conduction temperature difference of electronic components for all electronic components on the PCB board is as follows:

$$\Delta T_{cond} = (T_h - T_l) \tag{5}$$

In the equation, T_h represents the temperature of the PCB board, T_l represents the temperature of the electronic component.

According to the second law of thermodynamics, heat conduction follows a natural flow from high temperature to low temperature. During the process of constant current source power supply, power loss accumulates inside the chip in the form of thermal energy, becoming the main heat source. To accurately measure the thermal conductivity and avoid self-heating interference of electronic components, this paper innovatively proposes a separate measurement method: physically isolating the electronic components from the PCB board, connecting them only through wires, and directly testing the temperature of the soldering pad. Based on this new method, the expression of the temperature difference in heat conduction can be corrected to ensure the accuracy of the measurement results. Based on the new measurement method, the corrected expression of the temperature difference in heat conduction is:

$$\Delta T'_{cond} = \left(T_J - T_P\right) \tag{6}$$

In the equation, $\Delta T'_{cond}$ represents the temperature difference between the built-in constant current source chip and the electronic components, T_J represents the chip junction temperature, T_P represents the temperature of the electronic component solder pad.

In a steady-state system, energy follows the principle of conservation. For any heat source, the thermal power generated by it must be equal to the total heat power dissipated to the outside. When there are no other heat dissipation channels, heat conduction becomes the only heat dissipation method. Therefore, in this case, the self-heating power of the PCB board is equal to the power dissipated through heat conduction, that is, the two reach a state of equilibrium. The specific equation is as follows:

$$P_{origin\_t} = Q_{cond} \tag{7}$$

It can be derived from Equations (3), (4), (6) and (7)

$$\Delta T'_{cond} = \frac{(1-\eta)d}{kA} P_{origin\_in} \tag{8}$$

Since both η, d, k and A are constants, let the self-heating coefficient be $\alpha = \frac{(1-\eta)d}{kA}$. Then

$$\Delta T'_{cond} = \alpha P_{origin\_in} \tag{9}$$

The thermal resistance equation is a crucial theoretical tool in the fields of electronic engineering and thermal management, used to analyze and predict the temperature changes caused by power loss in electronic devices, chips, and systems during operation. The equation is as follows:

$$\Delta T_{self} = R_\theta P_{self\_t} \tag{10}$$

In the equation, ΔT_{self} represents the self-heating temperature rise, R_θ denotes the thermal resistance, and P_{self_t} signifies the power consumption of the electronic device itself. According to Equations (2) and (3):

$$\Delta T_{self} = R_\theta (1-\eta) P_{self\_in} \tag{11}$$

Since R_θ and η are constants, let the heat transfer coefficient be $\beta = R_\theta(1-\eta)$. Then

$$\Delta T_{self} = \beta P_{self\_in} \tag{12}$$

The impact of power on LED temperature is studied by examining the relationship between power and heat generation calculated through ADC and PWM. The modified relationship between heat generation Q and power P can be expressed as:

From Equations (9) and (12), we can obtain:

$$T = T_J + \beta P_{self\_in} - \alpha P_{origin\_in} \tag{13}$$

3. Construction of optical algorithm model

3.1. Color coordinates and luminous flux calibration

In the interior ambient lighting system, despite the slight differences in emission characteristics (wavelength and luminous intensity) among individual RGB LEDs, these minor variations can accumulate and amplify when a large number of LEDs are integrated into an application, significantly affecting the overall consistency of light color. To ensure uniformity of light color in the RGB ambient lighting system, precise calibration of color coordinates and luminous flux for each LED is crucial. Color coordinate calibration involves determining the exact position of LED emission on the chromaticity diagram, represented using the CIE 1931 chromaticity coordinates (x, y). Luminous flux calibration focuses on measuring the total luminous energy emitted by the LED, typically measured in lumens (lm). Through these two calibrations, specific

current PWM duty cycles can be set for each LED, ensuring consistency in output under specific light color requirements [16]. Given the inherent differences in wavelength and luminous intensity among LEDs of the same type, it is imperative to perform personalized color coordinate and luminous flux calibration for each RGB ambient light in order to achieve consistent light color. Considering that LED emission is achieved through the mixing of RGB three colors, it is necessary to dynamically calculate the color coordinates after mixing based on the set coordinate values to ensure precise and consistent final light color. The color coordinates after mixing can be obtained from Equations (14) and (15), as follows:

$$x_{target} = \frac{\frac{Y_{red}}{y_{red}} \times x_{red} \times R + \frac{Y_{green}}{y_{green}} \times x_{green} \times G + \frac{Y_{blue}}{y_{blue}} \times x_{blue} \times B}{\frac{Y_{red}}{y_{red}} \times R + \frac{Y_{green}}{y_{green}} \times G + \frac{Y_{blue}}{y_{blue}} \times B} \tag{14}$$

$$y_{target} = \frac{Y_{red} \times R + Y_{green} \times G + Y_{blue} \times B}{\frac{Y_{red}}{y_{red}} \times R + \frac{Y_{green}}{y_{green}} \times G + \frac{Y_{blue}}{y_{blue}} \times B} \tag{15}$$

$$Y_{target} = \frac{Y_{red} \times R + Y_{green} \times G + Y_{blue} \times B}{255} \tag{16}$$

In the equation, x_{target}, y_{target}, Y_{target}, denotes the color coordinates and luminous flux of the target color, x_{red}, y_{red}, x_{blue}, y_{blue}, x_{green}, y_{green} represent the color coordinates of the red, green, and blue chips, respectively; *R*, *G*, and *B* represent the preset color coordinates of the red, green, and blue chips, which are the command values for red, green, and blue in the LIN bus, The current luminous flux of the red, green, and blue LED chips is Y_{red}, Y_{green} and Y_{blue}.

The relationship between duty cycle, color coordinates, and luminous flux can be obtained from Equations (14)–(16), and the specific equations are as follows:

$$\begin{bmatrix} D_{red} \\ D_{green} \\ D_{blue} \end{bmatrix} = \begin{bmatrix} \frac{Y_{redLED}}{y_{redLED}} \times x_{redLED} & \frac{Y_{greenLED}}{y_{greenLED}} \times x_{greenLED} & \frac{Y_{blueLED}}{y_{blueLED}} \times x_{blueLED} \\ \frac{Y_{redLED}}{y_{redLED}} \times y_{redLED} & \frac{Y_{greenLED}}{y_{greenLED}} \times y_{greenLED} & \frac{Y_{blueLED}}{y_{blueLED}} \times y_{blueLED} \\ \frac{Y_{redLED}}{y_{redLED}} \times z_{redLED} & \frac{Y_{greenLED}}{y_{greenLED}} \times z_{greenLED} & \frac{Y_{redLED}}{y_{redLED}} \times z_{blueLED} \end{bmatrix}^{-1} \begin{bmatrix} x_{target} \\ y_{target} \\ z_{target} \end{bmatrix} \tag{17}$$

Among

$$z_{colour} = (1 - x_{colour} - y_{colour}) \tag{18}$$

In the equation D_{red}, D_{green} and D_{blue} represent the current duty cycles of the red, green, and blue chips, respectively, The color in z_{colour} represents the target, and red, green, and blue represent the differences between different parameters and the color coordinates of 1, which are used to calibrate the *x* and *y* color coordinates.

3.2. Color coordinate compensation strategy under temperature variation

3.2.1. Comprehensive mechanism of temperature and aging on the luminous characteristics of LEDs

In LED lighting systems, temperature and aging are two key factors that significantly affect the luminescence characteristics of LEDs. During operation, LED chips generate heat due to the passage of current, leading to an increase in junction temperature, which in turn affects their emission wavelength, luminous intensity, and color coordinates. Additionally, as the usage time extends, the aging of LED chip materials results in a decrease in light output efficiency and a shift in color coordinates. This aging effect varies under different temperature conditions, with a significantly accelerated aging rate in high-temperature environments. Therefore, to ensure the long-term stability of LED lighting systems, it is imperative to conduct in-depth research on the comprehensive mechanism of temperature and aging on the luminescence characteristics of LEDs.

3.2.2. Formulation and optimization process of compensation strategy

Benchmark measurement and data modeling

Firstly, under standard environmental conditions (such as in a 25 ℃ incubator), a high-precision integrating sphere is utilized to measure the reference color coordinates and luminous flux of red, green, and blue LED chips. Subsequently, through accelerated aging experiments, aging data of LED chips under different temperature conditions is obtained, and a multivariate mathematical model between luminous flux, temperature, and aging time is established. This model should be able to accurately describe the changes in luminescence characteristics of LEDs under different temperatures and aging states.

Real-time monitoring and condition assessment

Integrate high-precision temperature sensors and aging monitoring modules into LED lighting systems to monitor the operating temperature and cumulative working time (or cumulative luminous flux) of LED chips in real time. Based on the real-time monitoring data, utilize aging models to assess the current aging status of LED chips, providing accurate basis for subsequent color coordinate compensation.

Design and implementation of dynamic compensation algorithm

Based on the real-time monitored temperature and assessed aging state, the established mathematical model is utilized to dynamically calculate the color coordinate shift and luminous flux attenuation of the LED chip. Subsequently, an efficient dynamic compensation algorithm is designed to compensate for the color coordinate shift and luminous flux attenuation caused by temperature and aging in real time by adjusting the PWM signal duty cycle of the RGB channels, ensuring the consistency of light color under different working conditions of the LED lighting system.

System calibration and model update mechanism

To ensure the long-term effectiveness of the compensation strategy, it is necessary to regularly perform comprehensive calibration on the LED lighting system. By comparing the actual measured values with the model-predicted values, the accuracy of the compensation strategy is evaluated, and necessary corrections are

made to the model based on the calibration results. At the same time, with the continuous progress of LED chip technology and a deeper understanding of aging mechanisms, the aging model needs to be updated regularly to maintain the progressiveness and accuracy of the compensation strategy.

3.2.3. Optimization and implementation of compensation calculation equation

In the implementation process of color coordinate compensation strategy, more precise mathematical equations are required to calculate the color coordinate shift caused by temperature and aging. These equations should further introduce aging factors based on considering the impact of temperature, and dynamically correct the light decay coefficient. By programming these equations and combining with the hardware interface of the LED control system, real-time color coordinate compensation function can be achieved. At the same time, to improve compensation accuracy and response speed, advanced numerical calculation methods and optimization algorithms can be used to optimize the compensation process.

The specific calculation equation is as follows:

$$x'_{colourLED} = x_{colourLED} + x_{colourShift} \tag{19}$$

$$y'_{colourLED} = y_{colourLED} + y_{colourShift} \tag{20}$$

$$Y'_{colourLED} = Y_{colourLED} + Y_{colourShift} \tag{21}$$

In the equation $x_{colourLED}$ and $y_{colourLED}$ the subscripts *colour* in the text indicate that the color coordinates of red, green, and blue light are respectively represented by *red green* and *blue* at 25 ℃; $Y_{colourLED}$ and $Y'_{colourLED}$ represent the luminous flux at 25 ℃ and the luminous flux after temperature compensation, respectively; When the temperature changes, the compensated color coordinates are represented by $x'_{colourLED}$ and $y'_{colourLED}$;

$x_{colourShift}$, $y_{colourShift}$ and $Y_{colourShift}$ represent the *x* and *y* color coordinate offsets and luminous flux offset of the LED red color in the model at the current temperature.

Based on the data provided in the LED specification, **Figure 2** below illustrates the relationship between the luminous flux and temperature of the three internal chips in an RGB LED. In the figure, the horizontal axis represents the operating temperature of the chips, while the vertical axis indicates the ratio of the luminous flux of each chip at different temperatures to the luminous flux at 25 ℃. By analyzing the chart, it can be clearly observed that the luminous flux of the red chip is most significantly affected by temperature, exhibiting a large variation. This finding is of great significance for optimizing the performance of LEDs and ensuring their stability under different temperature conditions.

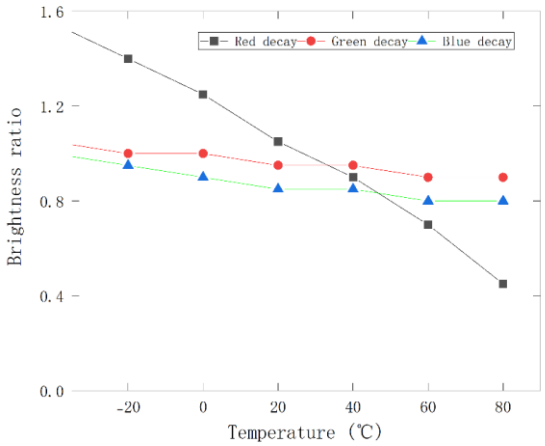

Figure 2. Relationship between temperature and luminous flux of red, green, and blue LED chips.

By applying the least squares method to the temperature-luminous flux relationship curve depicted in **Figure 2**, Equations (22)–(24) can be derived to describe the variation of luminous flux of RGB chips with temperature. Y_1, Y_2 and Y_3 represent the luminous decay of the red, green, and blue chips, respectively, which is the ratio of their luminous flux at a given temperature to that at 25 ℃; T_1, T_2 and T_3 represent the actual temperatures of the red, green, and blue chips, respectively. To accurately calculate the luminous flux variations of these three color chips, it is necessary to obtain temperature data using the temperature sensor on the ambient light circuit board, and then combine it with Equation (13) to determine the actual operating temperature of the RGB LED. This step provides a crucial basis for precise regulation of the LED's light output.

$$Y_1 = -0.007T_1 + 1.148 \tag{22}$$

$$Y_2 = -0.001T_2 + 1.009 \tag{23}$$

$$Y_3 = -0.001T_3 + 1.021 \tag{24}$$

When the temperature rises, the light decay values of the RGB three types of chips can be calculated using the previously derived Equations (20)–(22). To compensate for the color coordinate shift caused by light decay, it is necessary to adjust the current duty cycle of each color channel according to the rate of light decay attenuation, thus ensuring that the color coordinates remain consistent before and after temperature changes, and maintaining the stability and consistency of the light color. **Figure 3** visually demonstrates the color gamut distribution range of RGB LEDs under two temperature conditions of 25 ℃ and 85 ℃, highlighting the impact of temperature on light color performance and the necessity of compensation adjustment.

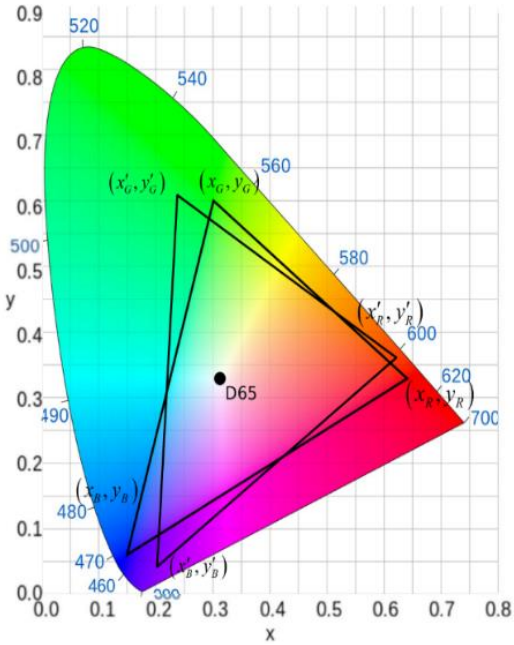

Figure 3. Yxy chromaticity and color gamut diagrams at 25 ℃ and 85 ℃.

4. Improve temperature prediction and optical compensation analysis of the PT-model

When the interior ambient lighting is operating, its temperature is significantly affected by power variations, which in turn impacts the self-heating power of the LED. To comprehensively evaluate the effectiveness and accuracy of the proposed temperature prediction model and optical algorithm model, based on the temperature model and optical algorithm model presented in this paper, two verification methods were adopted to predict temperature more accurately: point temperature line verification for actual surface temperature and optical integrating sphere verification for color coordinates and luminous flux.

4.1. LED temperature calculation

LED self-heating calculation

Due to the need to switch between different colors and brightness levels, the temperature of the interior ambient lighting is affected by power variations, thereby being influenced by self-heating power. The relationship between the self-heating temperature rise of the diode and the input power can be expressed as:

$$\Delta T_{Diode} = \beta_{Diode} P_{Diode\_in} \tag{25}$$

In the equation, ΔT_{Diode} represents the self-heating temperature rise, β_{Diode} denotes the self-heating coefficient of the diode, P_{Diode_in} represents the input power of the diode, and the equation is expressed as follows:

$$P_{Diode\_in} = V_{Diode} I_{Diode} \tag{26}$$

In the equation, V_{Diode} represents the diode voltage, which can be obtained through ADC, I_{Diode} represents the current. Since ambient lights typically feature three RGB LEDs, the equation is as follows:

$$I_{Diode} = I_r + I_g + I_b \tag{27}$$

In the equation, I_r represents the red light current, I_g represents the green light current, I_b represents the blue light current, and their calculation equation is as follows:

$$I_r = \frac{pwm_r}{pwm_{\max}} I_{\max} \tag{28}$$

$$I_g = \frac{pwm_g}{pwm_{\max}} I_{\max} \tag{29}$$

$$I_b = \frac{pwm_b}{pwm_{\max}} I_{\max} \tag{30}$$

In the equation, pwm_r, pwm_g, pwm_b The PWM values output for the RGB three channels of the chip can be obtained by reading the register, $pwm_{\max}$ represents the PWM period, $I_{\max}$ represents the peak current of the built-in constant current source in the chip.

Heat conduction calculation of MCU to LED pad

Due to the design of the ambient light using a chip MCU with an integrated constant current source, the power loss generated by the constant current source during the power supply process is mainly concentrated inside the chip in the form of heat. To accurately measure the impact of thermal conduction on the LED temperature, this paper proposes a new measurement method, which involves separating the electronic components from the PCB board and connecting them only through wires to test the temperature of the soldering pad. Based on the law of heat conduction, the temperature difference between the chip junction temperature and the LED soldering pad can be expressed as follows:

$$\Delta T_{MCU} = \alpha_{MCU} P_{MCU\_in} \tag{31}$$

In the equation, ΔT_{MCU} represents the temperature difference between the chip junction temperature and the LED pad temperature, while α_{MCU} denotes the thermal conductivity of the chip, P_{MCU_in} represents the input power of the MCU, Its expression can be represented as:

$$P_{MCU\_in} = V_{MCU} I_{MCU} \tag{32}$$

In the equation, V_{MCU} is the input voltage of the MCU, I_{MCU} represents the input current of the chip. Since it is in series, Therefore, V_{MCU} can be expressed as:

$$V_{MCU} = V_{BAT} - V_{Diode} \tag{33}$$

In the equation, V_{BAT} is the power supply voltage.

Computation of LED temperature integrated meter

By combining the self-heating effect of LEDs and the thermal conduction effect of MCU on the solder pad, this article derives a comprehensive temperature calculation equation for LEDs. Therefore, the temperature of the LED is:

$$T = T_J + \left(\beta V_{Diode} - \alpha(V_{BAT} - V_{Diode})\right) I_{\max} \frac{pwm_r + pwm_g + pwm_b}{pwm_{\max}} \quad (34)$$

4.2. Temperature model verification

4.2.1. Parameter measurement and experimental design

To verify the accuracy of the temperature prediction model, this paper designs a series of experiments. The actual temperatures of LEDs are measured under different ambient temperatures and compared with the model's prediction results. During the experiment, a separate measurement method is adopted, where the LED is separated from the PCB board and connected via wires to test the temperature of the soldering pad, in order to eliminate the interference of electronic component self-heating on thermal conductivity measurement, as shown in **Figure 4**. The experimental data are presented in **Tables 1–3**, covering the LED soldering pad temperature and LED temperature under different color channels and in the non-lighting state.

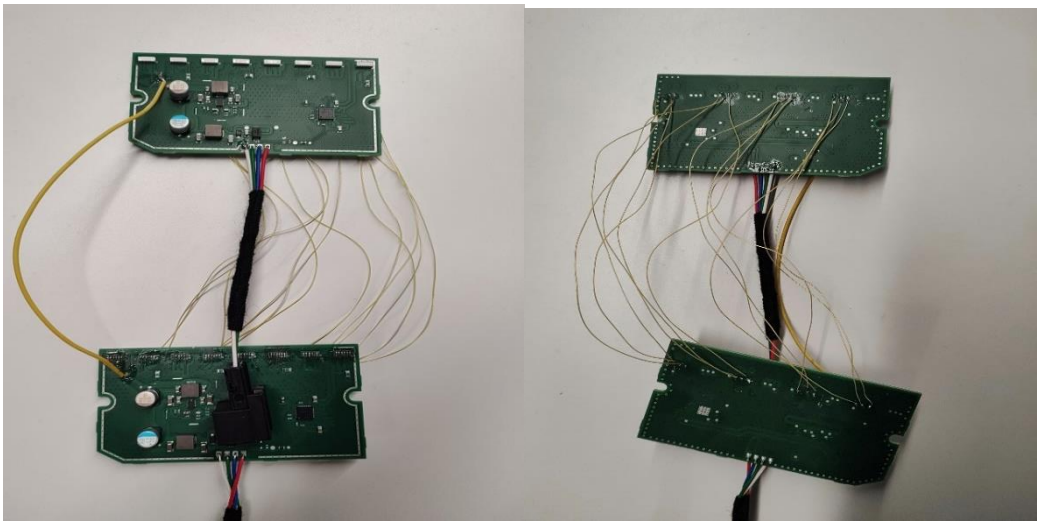

Figure 4. Test PCB experiment.

Temperature profile and equipment:

Table 1. Relevant data and test temperature data for PCB testing.

	Red	**Green**	**Blue**	**No light**
LED Pad Temperature	33.55	33.2	33.1	28.6
LED Temperature	27.2	26.95	26.65	25.3
V_r	1946			
V_g		2641		
V_b			2880	
PWM_r	13055			
PWM_g		13055		
PWM_b			13055	

Table 1. (*Continued*).

	Red	Green	Blue	No light
T_{mcu}	35.4	35.8	35.6	27.1
PWM_{max}	32000			
I_{max}	30			
Ambient Temperature	25			
V_s	11111			

Table 2. Measurement results of three-channel RGB LEDs.

	Single-point red	Single-point green	Single-point blue	No light
LED Pad Temperature	33.55	33.2	33.1	28.6
LED Temperature	27.2	26.95	26.65	25.3

Table 3. Calculation results of proportional coefficients.

Variable name	Numerical value
β	69.32787912
α	17.59818792

4.2.2. Analysis of experimental results

By incorporating the experimental data from **Tables 1** and **2** into the software program, we conducted a recompilation, generated a hex file, and programmed it into the chip. Subsequently, we conducted a temperature measurement experiment on the ambient lighting system and compared the measured temperatures with the predictions of the P-T model (a temperature prediction model based on constant current source output PWM). As shown in **Table 4**, the temperature model proposed in this paper significantly outperforms traditional models in prediction accuracy. Its prediction results are closer to the experimental measurements, with errors controlled within 4.3%. This result indicates that the improved P-T model exhibits high accuracy in predicting ambient lighting temperatures, thereby validating the model's effectiveness.

Table 4. Comparison between P-T model prediction results and test data.

Ambient temperature/℃	Test temperature/℃	PT prediction result/℃	Traditional prediction result/℃
−40	−33	−32.2	−28
−35	−28.2	−26.3	−22.7
−30	−23.1	−21.4	−17.9
−25	−17.4	−13.1	−10.6
−20	−13	−12.4	−9
−15	−7.4	−6.3	1.6
−10	−4.5	−3.3	−0.5
−5	0	2.9	2
0	4.6	6.9	15.6

Table 4. (*Continued*).

Ambient temperature/℃	Test temperature/℃	PT prediction result/℃	Traditional prediction result/℃
5	8.9	11	11.9
10	14.6	16.5	20.6
15	19.8	23.2	21.8
20	25.4	29.1	35.4
25	30.3	35.1	39.3
30	35.4	37.8	36.4
35	40	41.5	47
40	45.4	47.4	56.4
45	50.1	51.4	52.1
50	54.5	57.1	67.5
55	60.5	64.6	65.5
60	65.3	68.3	67.3
65	70.5	71.1	79.5
70	75.8	78.1	76.8
75	81.5	82.7	89.5
80	86.4	88.4	96.4
85	91.6	96.2	105.6
90	96	99.1	103
95	101.9	102.4	101.9
100	107.5	110	120.5
105	111.7	115.1	119.7
110	117.4	120.1	125.4
115	122.7	126.3	125.7
120	127.6	128.1	133.6

Specifically, the experimental data encompasses a wide range of ambient temperatures from −40 ℃ to 120 ℃. By comparing the model's predicted values with the actual experimental measurements, it was found that the P-T model's prediction errors at various temperature points are smaller than those of traditional models, and in most cases, the errors are significantly below the threshold of 4.3%. **Figure 5** visually demonstrates the comparison between predicted values and actual measurements, further confirming the superior performance of the P-T model in temperature prediction. This research not only provides a new method for enhancing the temperature prediction accuracy of ambient lighting systems but also lays a solid foundation for subsequent research on optical compensation algorithms.

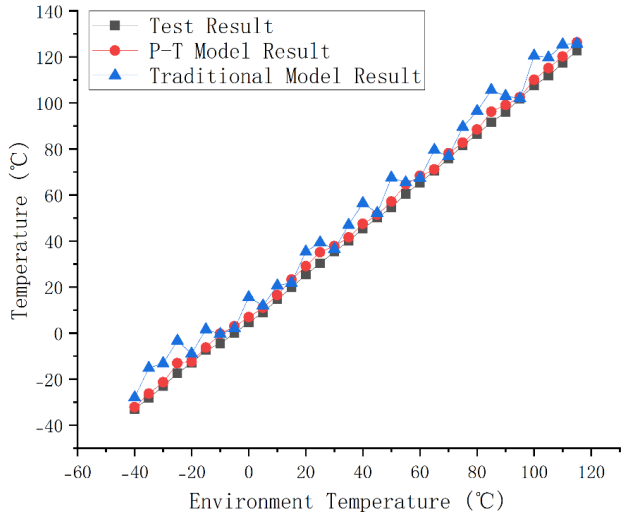

Figure 5. Comparison of ambient light temperature test results and model predictions.

4.3. Optical experiment verification

To further verify the effectiveness of the proposed optical algorithm model, this paper utilizes a high-precision optical integrating sphere as the experimental equipment. By precisely adjusting the signal values of the RGB channels, the integrating sphere achieves accurate reading of color coordinates for various colors. As shown in **Figure 6**, the integrating sphere performs exceptionally well in fatigue tests. During the experiment, comprehensive color coordinate measurements were conducted for the ambient lighting system, covering 30 different color combinations. Subsequently, the measurement results were thoroughly compared and analyzed with the predicted values based on traditional temperature models.

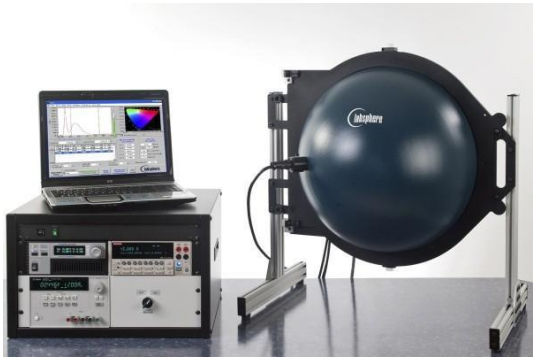

Figure 6. Integrating sphere test experiment.

DeltaUV, as a core parameter for evaluating the differences in color within the UV color space, plays a crucial role in assessing the consistency and stability of colors. To rigorously verify the effectiveness of the proposed improved temperature model, this paper first recompiled the software, generated the corresponding hex file, and reliably programmed it into the control chip. Subsequently, to ensure that the illumination output of the ambient lights meets predetermined standards, precise light calibration was performed to eliminate the impact of initial errors on subsequent experiments. On this basis, this paper meticulously designed a color coordinate measurement experiment involving 30 different colors, aiming to comprehensively

evaluate the predictive performance of the temperature model under various color conditions. During the experiment, standard operating procedures were strictly followed to ensure the accuracy and comparability of measurement data. Subsequently, a detailed comparative analysis was conducted between the color coordinates obtained from the experiment and the predicted values of the unimproved temperature model. As shown in **Tables 5** and **6**, as well as visually presented in **Figures 6** and **7**, the improved temperature model proposed in this paper demonstrates extremely high accuracy in predicting color coordinates. The error between its predicted results and standard color coordinates is strictly controlled within 0.0067, which significantly outperforms traditional models, thus effectively verifying the significant advantage of the improved temperature model in enhancing color prediction accuracy.

Table 5. PT model test results.

CIE1931		**CIE1976**		**Measurement**			**DeltaUV**
X	**Y**	**U**	**V**	**X**	**Y**	**L**	
0.3169	0.3310	0.2000	0.4700	0.313	0.3307	2.7090	0.0027
0.3197	0.3497	0.1950	0.4800	0.3193	0.3492	2.6890	0.0003
0.4016	0.5034	0.1950	0.5500	0.4099	0.5186	2.4490	0.0054
0.4165	0.4966	0.2050	0.5500	0.4242	0.5094	2.4450	0.0048
0.4310	0.4900	0.2150	0.5500	0.4376	0.5008	2.4140	0.0041
0.4576	0.4619	0.2400	0.5450	0.4659	0.4745	2.3710	0.0052
0.4959	0.4449	0.2700	0.5450	0.5012	0.4538	2.2880	0.0038
0.5289	0.4162	0.3050	0.5400	0.5349	0.4269	2.2270	0.0050
0.5532	0.3927	0.3350	0.5350	0.5604	0.4034	2.1590	0.0055
0.5897	0.3655	0.3800	0.5300	0.5964	0.3764	2.0650	0.0063
0.6846	0.3072	0.5150	0.5200	0.6885	0.3089	1.6810	0.0024
0.6540	0.2906	0.5050	0.5050	0.6707	0.2978	1.6490	0.0008
0.6282	0.2821	0.4900	0.4950	0.6387	0.289	1.6640	0.0065
0.5211	0.2316	0.4400	0.4400	0.5167	0.2336	1.6310	0.0067
0.2082	0.0680	0.2450	0.1800	0.2106	0.0706	1.1110	0.0055
0.1486	0.0288	0.1950	0.0850	0.1553	0.0336	0.9151	0.0034
0.1579	0.1053	0.1600	0.2400	0.157	0.1079	1.4410	0.0045
0.1586	0.1409	0.1450	0.2900	0.1577	0.143	1.6290	0.0030
0.1580	0.1664	0.1350	0.3200	0.1573	0.1691	1.7430	0.0032
0.1609	0.2060	0.1250	0.3600	0.1591	0.2086	1.9070	0.0031
0.1667	0.2407	0.1200	0.3900	0.1649	0.2424	2.0300	0.0021
0.1667	0.2828	0.1100	0.4200	0.164	0.2838	2.1410	0.0021
0.1766	0.3402	0.1050	0.4550	0.1782	0.3404	2.3110	0.0010
0.1800	0.3800	0.1000	0.4750	0.1826	0.3789	2.3920	0.0017
0.1808	0.4144	0.0950	0.4900	0.1826	0.4115	2.4580	0.0017

Table 5. (*Continued*).

CIE1931		CIE1976		Measurement			DeltaUV
X	Y	U	V	X	Y	L	
0.1861	0.5109	0.0850	0.5250	0.1885	0.5026	2.5900	0.0031
0.1934	0.6418	0.0750	0.5600	0.198	0.6635	2.7300	0.0052
0.2368	0.6205	0.0950	0.5600	0.243	0.6417	2.6790	0.0054
0.3092	0.5649	0.1350	0.5550	0.3178	0.5807	2.6140	0.0051
0.3696	0.5362	0.1700	0.5550	0.3777	0.5484	2.5180	0.0044

Table 6. Test results of traditional models.

CIE1931		CIE1976		Measurement			DeltaUV
X	Y	U	V	X	Y	L	
0.3169	0.3310	0.2000	0.4700	0.3135	0.3339	2.7090	0.0036
0.3197	0.3497	0.1950	0.4800	0.3218	0.3552	2.6890	0.0030
0.4016	0.5034	0.1950	0.5500	0.4183	0.5262	2.4490	0.0089
0.4165	0.4966	0.2050	0.5500	0.4269	0.5162	2.4450	0.0070
0.4310	0.4900	0.2150	0.5500	0.4412	0.5047	2.4140	0.0058
0.4576	0.4619	0.2400	0.5450	0.4664	0.4757	2.3710	0.0056
0.4959	0.4449	0.2700	0.5450	0.5058	0.4564	2.2880	0.0053
0.5289	0.4162	0.3050	0.5400	0.5378	0.4355	2.2270	0.0091
0.5532	0.3927	0.3350	0.5350	0.5617	0.4128	2.1590	0.0108
0.5897	0.3655	0.3800	0.5300	0.6021	0.3803	2.0650	0.0083
0.6846	0.3072	0.5150	0.5200	0.6909	0.3184	1.6810	0.0097
0.6540	0.2906	0.5050	0.5050	0.6802	0.3048	1.6490	0.0008
0.6282	0.2821	0.4900	0.4950	0.6469	0.2924	1.6640	0.0114
0.5211	0.2316	0.4400	0.4400	0.5212	0.2414	1.6310	0.0130
0.2082	0.0680	0.2450	0.1800	0.212	0.0773	1.1110	0.0188
0.1486	0.0288	0.1950	0.0850	0.162	0.0337	0.9151	0.0034
0.1579	0.1053	0.1600	0.2400	0.1604	0.1176	1.4410	0.0190
0.1586	0.1409	0.1450	0.2900	0.1641	0.1432	1.6290	0.0058
0.1580	0.1664	0.1350	0.3200	0.1616	0.1708	1.7430	0.0055
0.1609	0.2060	0.1250	0.3600	0.1641	0.2178	1.9070	0.0109
0.1667	0.2407	0.1200	0.3900	0.1736	0.2476	2.0300	0.0071
0.1667	0.2828	0.1100	0.4200	0.1648	0.2894	2.1410	0.0048
0.1766	0.3402	0.1050	0.4550	0.1858	0.3405	2.3110	0.0059
0.1800	0.3800	0.1000	0.4750	0.1904	0.3869	2.3920	0.0066
0.1808	0.4144	0.0950	0.4900	0.1914	0.4201	2.4580	0.0062
0.1861	0.5109	0.0850	0.5250	0.1969	0.5067	2.5900	0.0057
0.1934	0.6418	0.0750	0.5600	0.1983	0.67	2.7300	0.0066
0.2368	0.6205	0.0950	0.5600	0.2481	0.6506	2.6790	0.0080
0.3092	0.5649	0.1350	0.5550	0.3232	0.5851	2.6140	0.0073
0.3696	0.5362	0.1700	0.5550	0.3876	0.5503	2.5180	0.0082

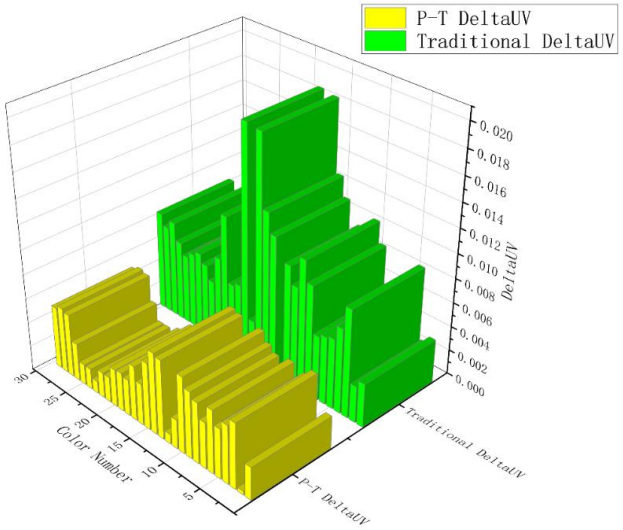

Figure 7. Comparison of optical test results between two models.

5. Conclusion

This article addresses the issue of color consistency in RGB-LED ambient lighting, proposing a temperature prediction model based on power that takes into account the self-heating effect of LEDs. Combined with optical algorithms, it achieves dynamic compensation for color coordinates and luminous flux. Experimental results show that the model's prediction error is below 4.3%, significantly outperforming traditional methods and effectively enhancing the color stability of LED ambient lighting under temperature variations. Furthermore, the model and algorithm have been validated on multiple vehicle models, demonstrating good practicality and promotional value, providing theoretical support for the optimization of interior lighting systems.

Author contributions: Conceptualization, LT and ML; methodology, LT; software, LT; validation, LT; formal analysis, ML; investigation, LT; resources, ML; data curation, LT; writing—original draft preparation, LT; writing—review and editing, ML; visualization, LT; supervision, LT; project administration, LT; funding acquisition, LT. All authors have read and agreed to the published version of the manuscript.

Ethical approval: Not applicable.

Conflict of interest: The authors declare no conflict of interest.

References

1. Zhang L, Dong FG, Sun XZ, et al. Color Adjustment Technology for RGB Atmosphere Lighting in Cars. China Lighting & Electric Appliance, 2017(8): p37–39.
2. Dong SJ. Design and Implementation of Automotive Ambiance Lighting Based on Musical Rhythm. Jiangxi: East China Jiaotong University, 2023.
3. L. Chen, K. Fu, Z. Jiang, Z. Wan and G. Wan, Research on Efficient RGB LEDs Color Parameter Error Prediction and Its High Accurate Calibration Method, in IEEE Transactions on Instrumentation and Measurement, vol. 71, pp. 1-11, 2022, Art no. 2512411, doi: 10.1109/TIM.2022.3186067.

4. Xie RP, Jin B, Yang Y, Yue XP. Experimental Study on the Dual-Heat-Source Thermal Model of pc-LEDs. Journal of Xihua University (Natural Science Edition), 2022, 41(4): P46–51.
5. Feng Z, Li Y, Xiao X, et al. Correlated color temperature control of multi-primary color LED lighting sources. Optics and Precision Engineering, 2015, 23(4): P926–933.
6. Vila O, Boada I, Raba D, Farres E. A Method to Compensate for the Errors Caused by Temperature in Structured-Light 3D Cameras. Sensors. 2021; 21(6):2073. https://doi.org/10.3390/s21062073
7. Moreno D, Rufo J, Guerra V, Rabadan J, Perez-Jimenez R. Effect of Temperature on Channel Compensation in Optical Camera Communication. Electronics. 2021; 10(3):262. https://doi.org/10.3390/electronics10030262
8. Jin R, Huan T, Xiao F. Nonlinear dynamic prediction model for color temperature of white LEDs. Journal of Luminescence, 2016, 37(1): P106–111.
9. Hui J-T, Xin H-Z, Jin Z. Optimization method for white light temperature spectrum of red/green/blue/warm white 4-color LEDs. Acta Optica Sinica, 2023, 43(9): 261–268.
10. Meng, H., Kong, F., & Li, K. (2022). Rapid calculation method to evaluate thermal management of LED systems based on an improved multi-layer model. Results in Physics, 43, 106046.
11. Li X. Mathematical and Numerical Modeling of Heat Distribution in LED Radiators. Zhejiang: Zhejiang University, 2016.
12. Liu, M., Li, W., Chen, W., Ibrahim, M. S., Xiong, J., Zhang, G., & Fan, J. (2024). Junction temperature and luminous flux prediction for white LED array based on electrical-photo-thermal modeling. Case Studies in Thermal Engineering, 54, 103940.
13. Zhang, L., Lu, F., Tao, G., Li, M., Yang, Z., Wang, A., ... & Wang, J. (2024). Prediction of Operational Lifetime of Perovskite Light Emitting Diodes by Machine Learning. Advanced Intelligent Systems, 2300772.
14. Wan G, et al. “A 3-D Finite Difference Method for Obtaining the Steady-State Temperature Field of a PCB Circuit.” IEEE Transactions on Power Electronics. 38 (2023): 2032–2040.
15. Bolzan TE, et al. “Improved methodology for predicting correlated color temperature in mixed LED lighting sources.” 2020 22nd European Conference on Power Electronics and Applications (EPE’20 ECCE Europe) (2020): P1–10.
16. Song PC, Wen SS, Jun S, et al. Method for dimming and color tuning of three-primary-color LEDs based on PWM. Acta Optica Sinica, 2015, 35(2): P285–292.